Eur Radiol (2009) 19: 1019–1024
DOI 10.1007/s00330-008-1213-5

NEURO

Yoshiyuki Watanabe
Kensuke Uotani
Tetsuro Nakazawa
Masahiro Higashi
Naoaki Yamada
Yoshiro Hori
Suzu Kanzaki
Tetsuya Fukuda
Toshihide Itoh
Hiroaki Naito

Dual-energy direct bone removal CT angiography for evaluation of intracranial aneurysm or stenosis: comparison with conventional digital subtraction angiography

Received: 6 June 2008
Revised: 11 August 2008
Accepted: 22 September 2008
Published online: 11 November 2008

Y. Watanabe · K. Uotani ·
T. Nakazawa · M. Higashi ·
N. Yamada · Y. Hori · S. Kanzaki ·
T. Fukuda · H. Naito
Department of Radiology,
National Cardiovascular Center,
Osaka, Japan

Y. Watanabe (✉)
Department of Radiology,
St. Luke's International Hospital,
9-1 Akashicho, Chuo-ku,
Tokyo, 104-8565, Japan
e-mail: yowatana@luke.or.jp
Tel.: +81-6-68335012
Fax: +81-6-68727486

T. Itoh
Siemens Asahi Medical Technologies,
Tokyo, Japan

Abstract Dual energy CT can be applied to bone elimination for cerebral CT angiography (CTA). The aim of this study was to compare the results of dual energy direct bone removal CTA (DE-BR-CTA). To those of DSA. Twelve patients with intracranial aneurysms and/or ICA stenosis were performed on a dual-source CT in dual energy mode. A post-processing software selectively remove bone structures using the two energy data sets. 3D-images with and without bone removal were reviewed and compared to DSA. Dual energy bone removal was successful in all patients. For 10 patients, bone removal was good and CTA MIP images could be used for vessel evaluation. For 2 patients, bone removal was moderate with some bone remnants but this did not disturb the 3D visualization. Three aneurysms adjacent to the skull base were only partially visible in conventional CTA but were fully visible in DE-BR-CTA. In 5 patients with ICA stenosis, DE-BR-CTA revealed the stenotic lesions on the MIP images. The correlation between DSA and DE-BR-CTA was good (R^2=0.822), but DE-BR-CTA lead to an overestimation of stenosis. DE-BR-CTA is able to eliminate bone structure using only a single CT data acquisition and is useful to evaluate intracranial aneurysms and stenosis.

Keyword Cerebral CTA · Dual-energy CT · Dual-source CT · Bone elimination · Brain

Introduction

Cerebral computed tomography angiography (CTA) has become a powerful, noninvasive diagnostic tool for evaluating cerebrovascular disease [1–3]. However, single-source CTA still has drawbacks compared to digital subtraction angiography (DSA), in particular for the evaluation of arteries with calcified plaque or vessels located next to the skull bone, as these vasculatures cannot be unambiguously distinguished from surrounding bony or calcified structures. This problem can be solved by applying subtracting CTA to a noncontrast and a contrast CT data set to eliminate bones [4–8]. Dual-source, dual-energy CT has the potential to distinguish iodine from bone or calcifications using the attenuation difference between the two energies [9].

Here, we evaluated the performance of dual-energy direct bone removal CTA (DE-BR-CTA) for diagnosing brain aneurysms, internal carotid artery (ICA) stenosis, or both. We also compared the DE-BR-CTA findings with those of DSA.

Materials and methods

Subjects

This study was performed after obtaining approval of the local institutional review board. Written informed consent was obtained from all patients. We prospectively selected 12 patients (7 male, 5 female; 36–78 years, mean 64 years) who underwent both DE-BR-CTA and DSA within 30 days of each other. Nine patients were suspected of intracranial unruptured aneurysms with MR angiography. Five patients were suspected of ICA stenosis. Of these five, three patients had a stroke and in two patients the asymptomatic stenosis was found during the evaluation for aneurysm.

CTA protocol

CTA was performed using a dual-source CT system (SOMATOM Definition, Siemens, Germany). CT parameters in the dual-energy mode were 140 and 80 kV tube voltage, 80 and 360 effective mAs, respectively, 0.5-s rotation time, 64×0.6-mm collimation with z-flying focal spot, and a pitch of 0.6. The 140 and 80 kV images (dual-energy images) were reconstructed separately in sections that were 0.75 mm wide at 0.5 mm increments using a D30 kernel for a field of view of 180 mm. Contrast material (350 mg I/ml) was injected for 20 s via the antecubital vein, followed by a 25 ml saline flush. Injection rate and dose depended on the patient's weight: 3.0 ml/s, 60 cc for patients weighing less than 60 kg; 3.5 ml/s, 70 cc for patients weighing less than 70 kg; and 4 ml/s, 80 cc for those over 70 kg. The delay time of the CT data acquisition after the injection was determined using a bolus tracking software at the basilar artery or ICA.

DSA was performed using a biplane DSA unit with rotational 3D DSA (INTEGRIS BV3000, Philips Healthcare, Best, Netherland).

Image processing and analysis

The dual-energy images were transferred to a workstation (Multi Modality Workplace; Siemens Medical Solutions, Germany), and the prototype of a commercial software (Syngo 2008G) was used to create a DE-BR-CTA from which the bone voxels had been removed ("head bone removal" application). The combined images of both energy data were reconstructed and used for diagnostic reading (conventional CTA).

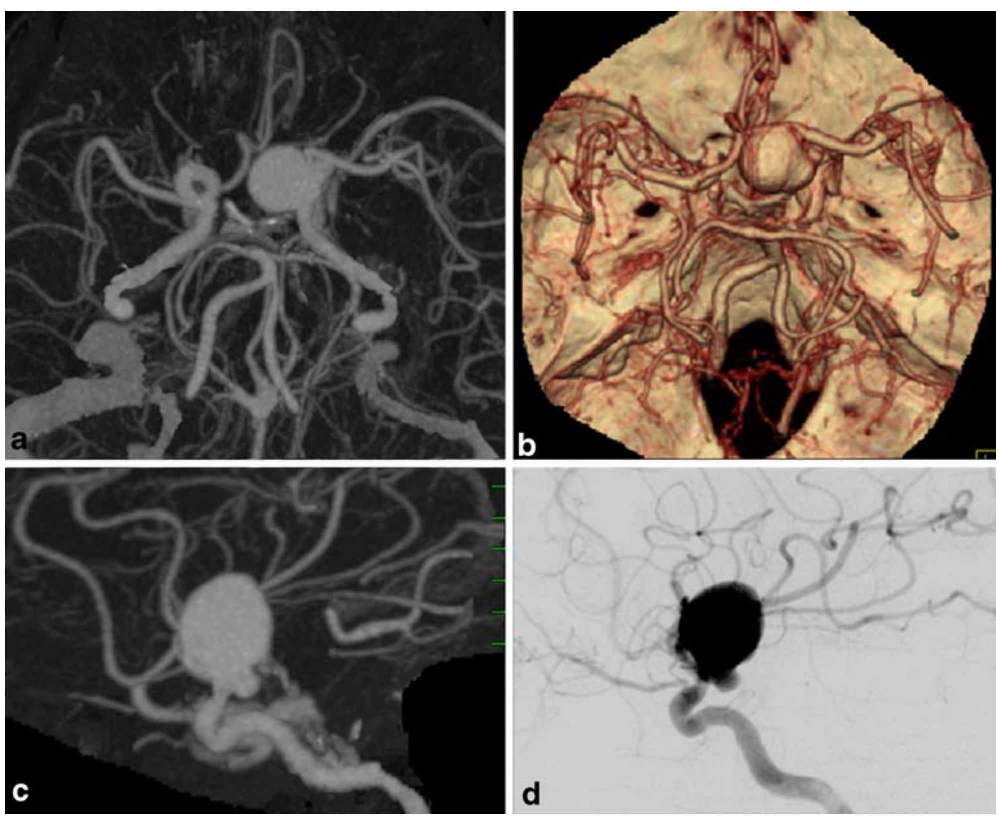

Fig. 1 Right ICA large aneurysm of a 75-year-old female patient. MIP images of DE-BR-CTA (**a**, **c**) delineate the general shape and configuration of aneurysm as well as DSA (**d**). VR image of conventional CTA (**b**) did not show the caudal side of aneurysm with bone

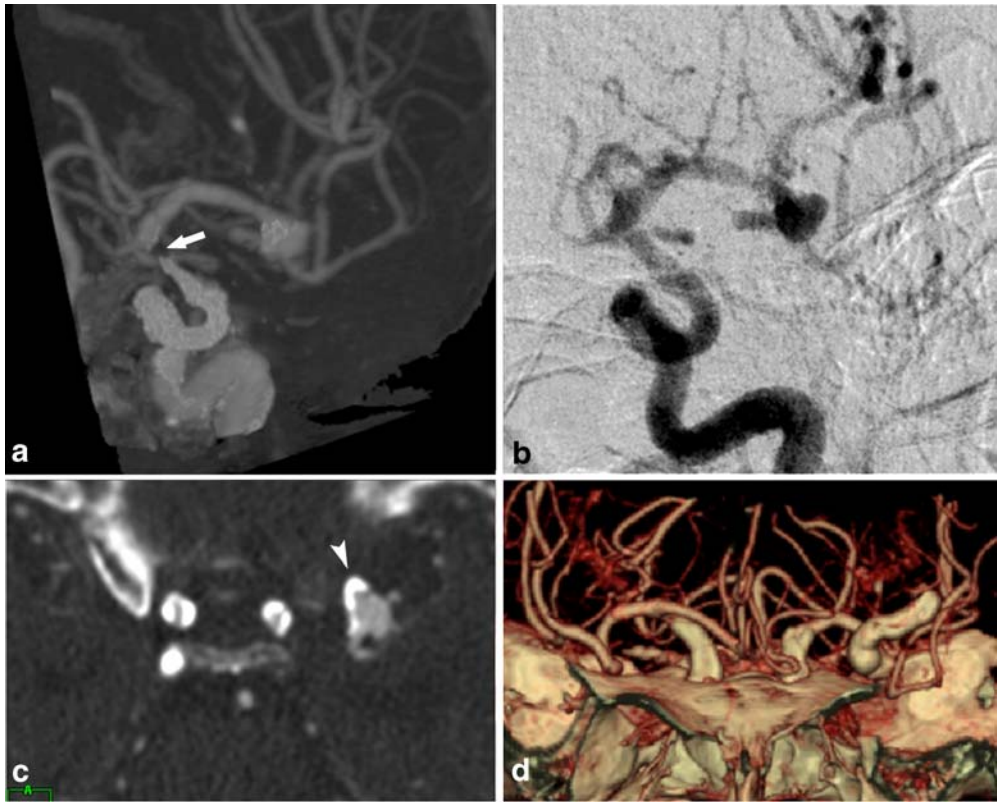

Fig. 2 Left MCA calcified aneurysm and bilateral ICA stenosis with hard plaque in a 77-year-old female patient. MIP image of DE-BR-CTA (**a**) removed the calcifications of ICA and aneurysm and revealed the same aneurysm shape as with DSA (**b**). However, the DE-BR-CTA (**a**) shows a short defect at the severe stenotic site at ICA terminal (*arrow*). CTA source images (**c**) show dense calcifications around the whole circumference of the ICA and anterior wall of the left MCA aneurysm (*arrowheads*). VR image of conventional CTA (**d**) showed the dense calcification at bilateral ICA and aneurysms, but failed to reveal details

Two neuroradiologists blinded to all clinical information independently reviewed the DE-BR-CTA in maximum-intensity projection (MIP) and the conventional CTA in volume-rendering (VR) technique on a 3D workstation. Disagreements regarding final conclusions were resolved by consensus.

The quality of the dual-energy bone removal was rated according to a four-point scale. “Excellent” was defined as clearly visible vasculature and no bone remnants, “good” as discernable vasculature and containing only tiny bone remnants, “moderate” as containing larger bone remnants that did not however disturb the vessel visualization, and

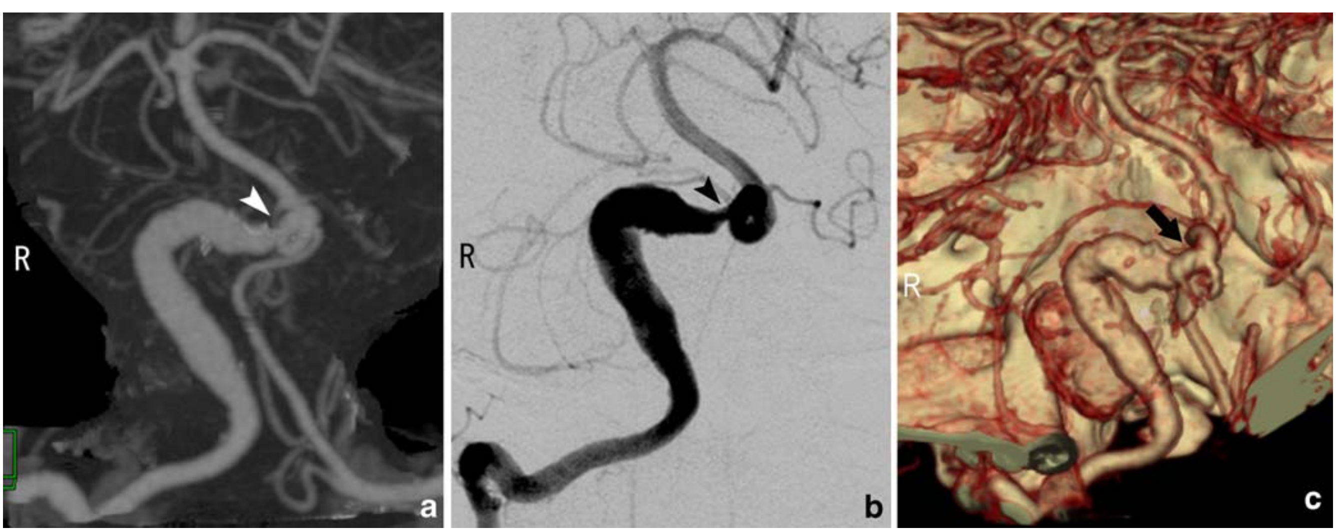

Fig. 3 Right vertebral artery fusiform aneurysm with calcification in a 55-year-old male patient. MIP image of DE-BR-CTA (**a**) removed the calcification of aneurysm and revealed the distal-end stenosis (*arrowhead*) of the aneurysm as with DSA (**b**). VR image of conventional CTA (**c**) showed the calcification (*arrow*), but the stenosis is hard to see

“poor” as including large bone remnants or artifacts covering parts of the vessels.

Further, the visibility of the ophthalmic artery in DE-BR-CTA was rated according to a four-point scale. “Excellent” was defined as the ophthalmic artery being visible from the origin to the intra-orbital portion, “good” as one artery being visible and the other with only the origin or other short segments being detected, “poor” as the long segment of the ophthalmic artery being detected, and “not visible” as the ophthalmic artery not being discernable at all.

For the evaluation of aneurysm, conventional CTA and DE-BR-CTA were compared for the detection and delineation of aneurysms and compared to the DSA results.

For the evaluation of ICA stenosis, the DE-BR-CTA and DSA were compared and the degree of stenosis was calculated using the Warfarin-Aspirin Symptomatic Intracranial Disease Study method [10], which is the ratio of the diameter of the maximum stenotic site to the diameter of the proximal normal ICA.

Kappa statistics were used to assess interobserver reliability. Kappa values above 0 were considered to indicate positive agreement: less than 0.4, positive but poor agreement; 0.41–0.75, good agreement; and more than 0.75, excellent agreement.

Results

Dual-energy bone removal was successful in all patients and the post-processing of DE-BR-CTA took an average of 53 s, excluding data transfer and saving time. The quality of dual-energy bone removal was rated “excellent” for two of the patients, “good” for eight patients, and “moderate” for two patients.

Of the 24 ophthalmic arteries, the visibility of 7 was rated “excellent,” 14 were rated “good,” 1 was rated “poor,” and 2 arteries were rated “not visible.” The two ophthalmic arteries that were not visible in DE-BR-CTA were found by DSA to be occluded. Interobserver reliability between two readers was good for quality of bone removal (k=0.60) and visibility of ophthalmic arteries (k=0.65).

Aneurysms were located in the vertebral artery (two patients), basilar artery (one patient), ICA (two patients),

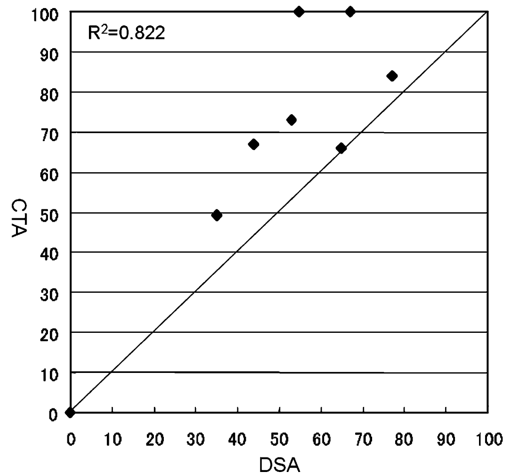

Fig. 5 Scatterplots illustrate percentages of carotid artery stenosis at DE-BR-CTA versus DSA. Good correlation was noted between the two methods (R^2=0.822), but the stenosis diagnosed by CTA was higher than that by DSA for most cases

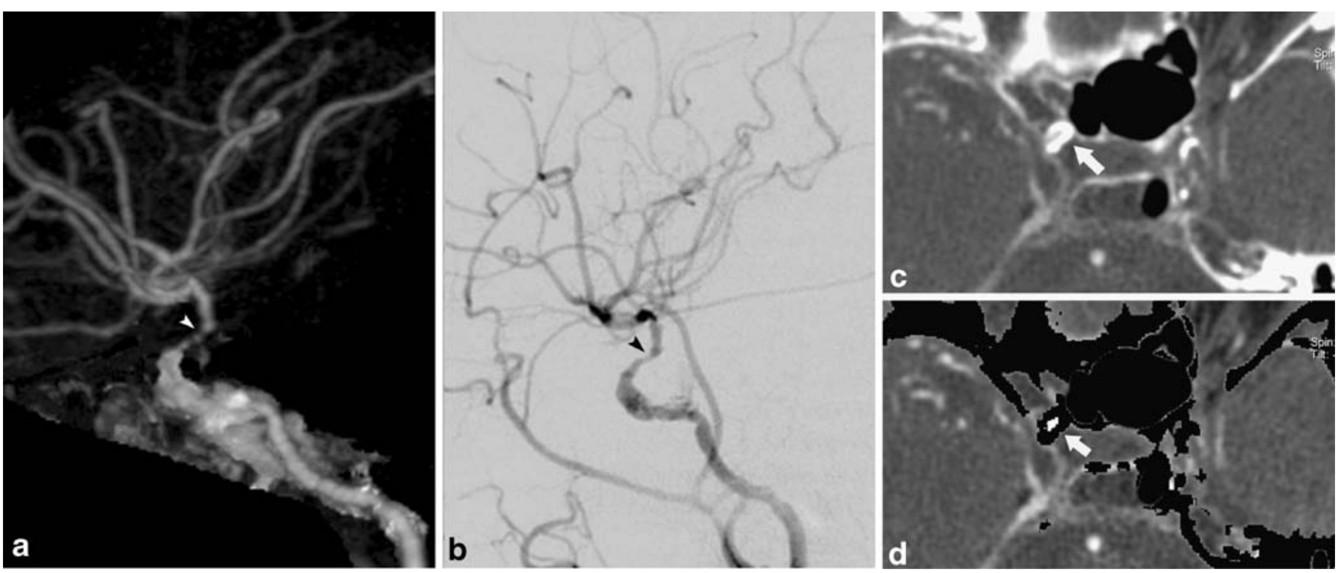

Fig. 4 Right ICA severe stenosis of a 67-year-old female patient. C2 portion of ICA had severe stenosis (*arrowhead*) demonstrated by DE-BR-CTA (**a**) and DSA (**b**). The ophthalmic artery is not visualized by DE-BR-CTA or by DSA. CTA source images (**c**) show dense calcifications around the whole circumference of the right ICA, and these calcifications were removed after DE bone-removal post-processing (**d**)

middle cerebral artery (MCA; three patients) and anterior communicating artery (ACOM; one patient).

Three aneurysms (two ICA and one MCA) adjacent to the skull base were only partially visible in conventional CTA but were fully visible in DE-BR-CTA (Fig. 1). For three aneurysms with calcifications [two MCA and one vertebral artery (VA)], the calcifications were removed by the head bone removal applications, and the intraluminal shape of the aneurysms was visualized precisely with results confirmed by DSA (Figs. 2, 3).

In five patients with ICA stenosis by calcification at the intercavernous or paraclinoid portion, the eight stenotic lesions were not visible in conventional CTA. However, after bone removal post-processing with dual energy, all stenotic lesions became clearly visible on the MIP images (Figs. 2, 4). The agreement of percent stenosis for the two methods is represented in the scatterplots shown in Fig. 5. The correlation between DSA and CTA was good (R^2= 0.822), and the majority of discordant points were above the line of correlation, indicating an overestimation of stenosis found on DE-BR-CTA compared to DSA.

Discussion

Our study shows that bone removal brain CTA using dual-energy data was useful to evaluate aneurysms and ICA stenosis with a short calculating time, and the results with DE-BR-CTA were comparable to those with DSA.

Dual-energy CT was developed during the late 1970s for tissue characterization using single-source, single-slice CT [11, 12] and mainly applied for bone densitometries [13, 14]. However, the limitation of CT hardware and software technology hampered expansion to further clinical applications [15].

Dual-source CT with dual-energy mode can acquire two different energy data into a single acquisition. Dual-energy CT imaging makes it possible to differentiate between certain materials, since X-ray absorption is material specific and dependent on the energy of the X-rays. Dual-energy CT for tissue characterization was reported for urinary stone differentiation [16–18], visualization of the knee ligament [19], and differentiation of iodine from bone and calcification [9].

Multi-slice CTA has a high sensitivity and specificity for the detection of intracranial aneurysm [1, 20].

Subtraction methods for bone removal in cerebral CTA have been reported for the evaluation of skull base aneurysm or extracranial ICA, such as simple subtraction from enhanced data to noncontrast data [4, 21]. More recently, selective bone removal or "matched mask bone elimination" have been widely used for bone-subtraction CTA where the bone mask image as well as the 3D registration to the enhanced CT acquisition were determined by a low-dose unenhanced CT acquisition [6–8].

In our study, DE-BR-CTA removed the bone structures very well, and the three aneurysms adjacent to the skull base were fully visible from all directions, in contrast to the partial view in conventional CTA.

Calcification of the aneurysmal wall makes surgical clipping difficult, so this information was important for deciding treatment strategies [22]. Conventional CTA images revealed calcifications but neither VR nor MIP images allowed a precise evaluation of the intraluminal aneurysmal shape. By comparison, the geometry of intraluminal aneurysms was clearly visible on DSA, yet calcifications could not be displayed. We found that calcifications of three aneurysms were removed by dual-energy bone removal, therefore the wall and luminal information of the aneurysms could be analyzed with both DE-BR-CTA and conventional CTA.

The advantage of the dual-energy bone removal method compared to CT digital subtraction methods is that it avoids the additional preliminary unenhanced CT acquisition. Single data acquisition reduces the radiation dose to the patient and also shows no misregistration artifacts. Subtraction methods use position adjustment, but if a patient moves between the two consecutive acquisitions, it becomes difficult to achieve a perfect match between the two images.

For the evaluation of intracranial stenosis and occlusion, DSA has been considered the reference standard [10]. The correlation between degree of intracranial stenosis based on CTA and DSA was excellent [23], and CTA has a higher sensitivity and positive predictive value than MRA [24]. Evaluation of ICA stenosis at the petrosal portion of carotid siphon or in cases of calcified plaque has not been reported previously, because CTA did not allow 3D visualization of ICA with these conditions. In contrast, DE-BR-CTA removed bone and calcifications and was able to measure the degree of stenosis.

As described above, we quantitatively evaluated ICA stenosis on MIP image. The correlation coefficient between DE-BR-CTA and DSA results was good, but stenosis tends to be overestimated in DE-BR-CTA compared to DSA. In our study, two severe stenotic arteries were misclassified as occluded (100% stenosis) with DE-BR-CTA. The main reason for this overestimation is blooming effects from calcifications. The poor enhancement of an artery with severe stenosis compared to a nonstenotic artery also makes it difficult to draw a clear demarcation between calcification and iodine. This problem might be resolved by optimization of demarcation parameters and reconstruction kernel.

Conclusion

Dual-energy bone removal using dual-source CT is able to eliminate bone and calcification from CTA images using only a single contrast-enhanced scan. DE-BR-CTA is a useful tool to evaluate intracranial aneurysms and stenosis.

References

1. Agid R, Lee SK, Willinsky RA et al (2006) Acute subarachnoid hemorrhage: using 64-slice multidetector CT angiography to “triage” patients’ treatment. Neuroradiology 48(11):787–794
2. Hashimoto H, Iida J, Hironaka Y et al (2000) Use of spiral computerized tomography angiography in patients with subarachnoid hemorrhage in whom subtraction angiography did not reveal cerebral aneurysms. J Neurosurg 92(2):278–283
3. Hirai T, Korogi Y, Ono K et al (2001) Preoperative evaluation of intracranial aneurysms: usefulness of intraarterial 3D CT angiography and conventional angiography with a combined unit-initial experience. Radiology 220(2):499–505
4. Jayakrishnan VK, White PM, Aitken D et al (2003) Subtraction helical CT angiography of intra- and extracranial vessels: technical considerations and preliminary experience. AJNR Am J Neuroradiol 24(3):451–455
5. Lell M, Anders K, Klotz E et al (2006) Clinical evaluation of bone-subtraction CT angiography (BSCTA) in head and neck imaging. Eur Radiol 16(4):889–897
6. Sakamoto S, Kiura Y, Shibukawa M et al (2006) Subtracted 3D CT angiography for evaluation of internal carotid artery aneurysms: comparison with conventional digital subtraction angiography. AJNR Am J Neuroradiol 27 (6):1332–1337
7. Tomandl BF, Hammen T, Klotz E et al (2006) Bone-subtraction CT angiography for the evaluation of intracranial aneurysms. AJNR Am J Neuroradiol 27 (1):55–59
8. Venema HW, Hulsmans FJ, den Heeten GJ (2001) CT angiography of the circle of Willis and intracranial internal carotid arteries: maximum intensity projection with matched mask bone elimination-feasibility study. Radiology 218(3):893–898
9. Johnson TR, Krauss B, Sedlmair M et al (2007) Material differentiation by dual energy CT: initial experience. Eur Radiol 17(6):1510–1517
10. Samuels OB, Joseph GJ, Lynn MJ et al (2000) A standardized method for measuring intracranial arterial stenosis. AJNR Am J Neuroradiol 21(4):643–646
11. Chiro GD, Brooks RA, Kessler RM et al (1979) Tissue signatures with dual-energy computed tomography. Radiology 131(2):521–523
12. Millner MR, McDavid WD, Waggener RG et al (1979) Extraction of information from CT scans at different energies. Med Phys 6(1):70–71
13. Genant HK, Boyd D (1977) Quantitative bone mineral analysis using dual energy computed tomography. Invest Radiol 12(6):545–551
14. Laval-Jeantet AM, Cann CE, Roger B et al (1984) A postprocessing dual energy technique for vertebral CT densitometry. J Comput Assist Tomogr 8(6):1164–1167
15. Kelcz F, Joseph PM, Hilal SK (1979) Noise considerations in dual energy CT scanning. Med Phys 6(5):418–425
16. Primak AN, Fletcher JG, Vrtiska TJ et al (2007) Noninvasive differentiation of uric acid versus non-uric acid kidney stones using dual-energy CT. Acad Radiol 14(12):1441–1447
17. Scheffel H, Stolzmann P, Frauenfelder T et al (2007) Dual-energy contrast-enhanced computed tomography for the detection of urinary stone disease. Invest Radiol 42(12):823–829
18. Graser A, Johnson TR, Bader M et al (2008) Dual energy CT characterization of urinary calculi: initial in vitro and clinical experience. Invest Radiol 43 (2):112–119
19. Sun C, Miao F, Wang XM et al (2008) An initial qualitative study of dual-energy CT in the knee ligaments. Surg Radiol Anat 30(5):443–447
20. Pozzi-Mucelli F, Bruni S, Doddi M et al (2007) Detection of intracranial aneurysms with 64 channel multidetector row computed tomography: comparison with digital subtraction angiography. Eur J Radiol 64(1):15–26
21. Gorzer H, Heimberger K, Schindler E (1994) Spiral CT angiography with digital subtraction of extra- and intracranial vessels. J Comput Assist Tomogr 18(5):839–841
22. Hoit DA, Malek AM (2006) Fusion of three-dimensional calcium rendering with rotational angiography to guide the treatment of a giant intracranial aneurysm: technical case report. Neurosurgery 58(1 Suppl):173–174
23. Nguyen-Huynh MN, Wintermark M, English J et al (2008) How accurate is CT angiography in evaluating intracranial atherosclerotic disease? Stroke 39 (4):1184–1188
24. Bash S, Villablanca JP, Jahan R et al (2005) Intracranial vascular stenosis and occlusive disease: evaluation with CT angiography, MR angiography, and digital subtraction angiography. AJNR Am J Neuroradiol 26(5):1012–1021